Soluble Electroluminescent Poly(phenylene vinylene)s with Balanced Electron- and Hole Injections

Yuh-Zheng Lee,[†] Xiwen Chen,[†] Show-An Chen,*[,†] Pei-Kuen Wei,[‡] and Wun-Shain Fann[‡]

Contribution from the Chemical Engineering Department, National Tsing-Hua University, Hsinchu, 30043, Taiwan, Republic of China, and Institute of Atomic and Molecular Sciences, Academia Sinica and Department of Physics, National Taiwan University, P.O. Box 23-166, Taipei, 106, Taiwan, Republic of China

Received August 22, 2000

Abstract: We report a new route for the design of efficient soluble electroluminescent PPV-based copolymers bearing electron-deficient oxadiazole (OXD) moieties on side chains. The introduction of OXD through a long alkylene spacer with PPV backbone provides a molecular dispersion of OXD in the film; both the side chain OXD and the main chain PPV do retain their own electron-transport and emissive properties, respectively. The use of phenylene vinylene derivatives with asymmetric and branched substituents and a long spacer provides solubility for ease of device fabrication as well as amorphous structure to allow a well-mixing of OXD groups with the main chains. By properly adjusting the OXD content through copolymerization, we can tailor the chemical structure of electroluminescent material to give a balance of hole- and electron injections for various metal cathodes, such that the quantum efficiency is significantly improved and the turn-on voltage is reduced for the devices with aluminum and calcium. For the device with calcium fabricated in open air, a maximum brightness of 15000 cd/m^2 at 15 V/100 nm and a maximum luminance efficiency of 2.27 cd/A can be obtained, respectively, about 30 times brighter and 9.4 times more efficient than those with the corresponding homopolymer, poly[2-methoxy-5-(2′-ethylhexyloxy)-*p*-phenylenevinylene] (MEH−PPV). The use of physical blends to simulate the copolymers provides no significant improvement, since phase-separation structures appear, causing an inefficient utilization of OXD and sometimes voltage-dependent emission spectra. The present route permits a fabrication of single layer PLED with high brightness, high efficiency, and low turn-on voltage.

Introduction

Polymer light-emitting diodes (PLEDs) have been studied extensively since the discovery that conjugated polymers can be used as the electroluminescent materials.[1] They possess many advantages over inorganic electroluminescence materials, such as low cost, easy processability, ease of forming large area, and mechanical flexibility.[2] In addition, the emissive color of PLEDs can be varied more easily than that of inorganic LEDs by proper selection of the wide varieties of luminescent materials. Among the vast kinds of conjugated polymers,[3] the most studied series is poly(phenylene vinylene)s (PPVs) due to their excellent luminescent and mechanical properties. By proper modification of the chemical structure, the fluorescent color of PPVs can span over visible color and further into the near-infrared region.

For commercialization of PLEDs, besides long lifetime, high quantum efficiency of the device is also an important issue, especially for passive driving display.[4] However, most of PPVs are good hole-transport material[5] with a low hole-injection barrier (except for those modified with an electron-withdrawing group, such as cyano-substituted PPV (CN−PPV)[6]), resulting in an imbalance of opposite carrier currents and a shift of the recombination zone toward the region near the interface of polymer/cathode and therefore in a lowering of the device efficiency due to quenching of excitons by the metal electrode. The effective methods that have been developed thus far for improving the quantum efficiency by balancing injected electrons and holes are adding an electron transport layer (ETL), which is commonly used in organic light-emitting diodes (OLED),[7] or using a blend of emissive polymer with charge-transport material as active layer.[8] In the former case, the ETL can be a thin layer of: (1) electron-transport molecular material having heterocyclic moiety such as 2-(4-biphenylyl)-5-(4-*tert*-butylphenyl)-1,3,4-oxadiazole, PBD,[9] (2) a blend of electron-transport molecular material with inert polymer such as poly-

* Corresponding author. E-mail: sachen@che.nthu.edu.tw.
[†] National Tsing-Hua University.
[‡] National Taiwan University.

(1) Burroughes, J. H.; Bradley, D. D. C.; Brown, A. R.; Marks, R. N.; MacKay, K.; Friend, R. H.; Burn, P. L.; Holmes, A. B. *Nature* **1990**, *347*, 539.

(2) Gustafsson, G.; Cao, Y.; Treasy, G. M.; Klavetter, F.; Colaneri, N.; Heeger, A. J. *Nature* **1992**, *357*, 477.

(3) (a) Kraft, A.; Grimsdale, A. C.; Holmes, A. B. *Angew. Chem., Int. Ed.* **1998**, *37*, 402. (b) Friend, R. H.; Gymer, R. W.; Holmes, A. B.; Burroughes, J. H.; Marks, R. N.; Taliani, C.; Bradley, D. D. C.; Dos Santos, D. A.; Brédas, J. L.; Logdlund, M.; Salaneck, W. R. *Nature* **1999**, *397*, 121.

(4) Johnson, M. J.; Sempel, A. *Inf. Disp.* **2000**, *2*, 12.

(5) (a) Takiguchi, T.; Park, D. H.; Yoshino, K. *Synth. Met.* **1987**, *17*, 657. (b) Meyer, H.; Haarer, D.; Naarmann, H.; Hörhold, H. H. *Phys. Rev. B* **1995**, *52*, 2587. (c) Blom, P. W. M.; de John, M. J. M.; Vleggaar, J. J. M. *Appl. Phys. Lett.* **1996**, *68*, 3308. (d) Martens, H. C. F.; Huiberts, J. N.; Blom, P. W. M. *Appl. Phys. Lett.* **2000**, *77*, 1852.

(6) (a) Greenham, N. C.; Moratti, S. C.; Bradley, D. D. C.; Friend, R. H.; Holmes, A. B. *Nature* **1993**, *365*, 628. (b) Grimsdale, A. C.; Cacialli, F.; Grüner, J.; Li, X.-C.; Holmes, A. B.; Moratti, S. C.; Friend, R. H. *Synth. Met.* **1996**, *76*, 165.

(7) Adachi, C.; Tsutsui, T.; Saito, S. *Appl. Phys. Lett.* **1989**, *55*, 1489. (b) Adachi, C.; Tsutsui, T.; Saito, S. *Appl. Phys. Lett.* **1990**, *56*, 799. (c) Adachi, C.; Tsutsui, T.; Saito, S. *Appl. Phys. Lett.* **1990**, *57*, 531. (d) Ohmori, Y.; Uchida, M.; Morishima, C.; Fujii, A.; Yoshino, K. *Jpn. J. Appl. Phys.* **1993**, *32*, L1663. (e) Takada, N.; Tsutsui, T.; Saito, S. *Appl. Phys. Lett.* **1993**, *63*, 2032. (f) Bettenhausen, J.; Strohriegl, P. *Adv. Mater.* **1996**, *8*, 507. (g) Bettenhausen, J.; Strohriegl, P.; Brütting, W.; Tokuhisa, H.; Tsutsui, T. J. *Appl. Phys.* **1997**, *82*, 4957.

10.1021/ja003135d CCC: $20.00
Published on Web 02/14/2001

(methyl methacrylate) (PMMA),[10] (3) an inert polymer such as poly(methacrylate) (PMA) having side chains comprising high electronegative heterocyclic moieties,[11] and (4) a conjugated or nonconjugated polymer having high electronegative heterocyclic moieties such as oxadiazole[12a−e], triazole,[12f] triazine,[12g,h] and quinoxaline[12i−k] on the main chains. However, the multilayer device always results in an unfavorable increase in turn-on voltage and requires careful selection of material and solvent to avoid damage of the emission layer by spin-coating an ETL. In the latter case involving a blend, a variation in emissive color with voltage[8a] and phase separation during storage and operation[12d] might occur, especially for that with molecular materials, in which the generated joule heat during the operation could accelerate a rate of recrystallization causing a reduction of the device stability.

A use of low work function metal as the cathode (such as calcium, magnesium, lithium) of PLEDs is an alternative to improving the device performance.[13] Due to matching the energy levels of the cathodes with the lowest unoccupied molecular orbitals (LUMO) of PPVs, amounts of injected electrons increase, and the brightness and quantum efficiency of PLEDs are improved. Although the mobility of electrons is higher than that of holes by 1 order of magnitude in a single MEH−PPV chain,[14] a recent report[5c,d] demonstrated that the presence of electron traps in the bulk film leads to a dramatic decrease in electron mobility. This leads to a reversal of the sequence of the mobilities, and the bulk film is regarded as trap-free for hole transport, and the electric behavior of the hole-only device shows space-charge limited current (SCLC) characteristics.[5c] Thus, the introduction of low work function metals still results in a device with imbalanced charge transport, and the improvement of electroluminescent efficiency is limited. Consequently, some efforts have been devoted to a molecular design of fluorescent materials and a modification of device architecture.

For the molecular design aspect, many efforts have been attempted to develop new emissive materials with improved electron-transport capability to allow a fabrication of efficient single-layer devices and for simplifying the fabrication process. For such purposes, heterocyclic aromatic moieties containing C═N segments with high electronegative properties have been incorporated into polymer main chains or side chains. For single-layer PLEDs, we and others have introduced electron-transport moieties on side chains, including electronegative moieties connecting by a short divalent spacer with PPV backbone[15] or directly attaching to the backbone[16] (i.e., conjugation with the main chain) or to a conventional polymer grafted with a phenylene vinylene luminescent segment[11a,17] or on the main chain having phenylene vinylene units,[18a−d] phenylene units[18e,f] or thiophene units.[18g] PLEDs fabricated therewith with Al as cathode have quantum efficiency improved by 1 order of magnitude as compared with those of corresponding polymers without the electron-transport moieties. As calcium is used as the cathode, either there is no improvement, or only slight improvement is observed. The incorporation of this kind of moiety into the conjugated main chains can affect the emissive spectrum;[16,18] as this also happened in small organic electroluminescent molecules by the formation of exciplex,[19] the role of the electron-transport moiety on the charge transport property is complicated and cannot be accessed easily. For devices with nonconjugated polymers grafted with both a luminescent segment and a high electronegative moiety as emissive materials, high operating voltage and poor operating life have resulted.[17a] Thus, to understand a way by which molecular design can provide a new material with a balanced charge transport at the desired emission color for any cathode material is necessary.

Here, we report a new series of soluble efficient electroluminescent PPV-based copolymers, which provides a balanced electron- and hole transport at various levels. The quantum efficiency is significantly improved, and the turn-on voltage is reduced for the device with aluminum or calcium as the cathodes. A series of new soluble random phenylene vinylene copolymers having the two co-repeat units, 2-methoxy 5-(2′-ethylhexyloxy) phenylene vinylene (MEHPV)[20] and 2-(10′-(*p*-(5″-phenyl-1″,3″,4″-oxadiazole-2″-yl) phenoxy) decanoxy) phenylene vinylene (POPDPV) is synthesized. The design is based on the consideration that the PPV backbone is a good hole-transporting electroluminescent material, the branched alkoxy side group provides solubility and prevention from crystallization, and the electron- deficient moiety, 2,5-diphenyl-1,3,4-oxadiazole-diyl (OXD), with flexible spacer of sufficient length as the side chain of POPDPV units, provides a highly improved electron-transporting property due to intrachain interaction and efficient mixing between OXD moieties with chromophores on

(8) (a) Uchida, M.; Ohmori, Y.; Noguchi, T.; Ohnishi, T.; Yoshino, K. Jpn. *J. Appl. Phys.* **1993**, *32*, L921. (b) Zhang, C.; Höger, S.; Pakbaz, K.; Wudl, F.; Heeger A. J. *J. Electron. Mater*. **1994**, *23*, 453. (c) Cimrová V.; Neher, D.; Remmers, M.; Kmínek, I. *Adv. Mater*. **1998**, *10*, 676. (d) Cao, Y.; Parker, I. D.; Yu, G.; Zhang, C.; Heeger, A. J. *Nature* **1999**, *397*, 414.

(9) Brown, A. R.; Bradley, D. D. C.; Burroughes, J. H.; Friend, R. H.; Greenham, N. C. *Appl. Phys. Lett.* **1992**, *61*, 2793. (b) Berggren, M.; Gustafsson, G.; Inganäs, O.; Anderson, M. R.; Hjertberg, T.; Wennerström, O. J. *Appl. Phys.* **1994**, *76*, 7530.

(10) Aratani, S.; Zhang, C.; Pakbaz, K.; Höger, S.; Wudl, F.; Heeger, A. J. *J. Electron. Mater*. **1993**, *22*, 745.

(11) (a) Li, X.-C.; Cacialli, F.; Giles, M.; Grüner, J.; Friend, R. H.; Holmes, A. B.; Moratti, S. C.; Yong, T. M. *Adv. Mater.* **1995**, *7*, 898−900. (b) Morgado, J.; Grüner, J.; Walcott, S. P.; Yong, T. M.; Cervini, R.; Moratti, S. C.; Holmes, A. B.; Friend, R. H. *Synth. Met.* **1998**, *95*, 113.

(12) (a) Yang, Y.; Pei, Q. J. *Appl. Phys*. **1995**, *77*, 4807. (b) Buchwald, E.; Meier, M.; Karg, S.; Pösch, P.; Schmidt, H.-W.; Strohriegl, P.; Rieb, W.; Schwoerer, M. *Adv. Mater.* **1995**, *7*, 839. (c) Strukelj, M.; Papadimitrakopoulos, F.; Miller, T. M.; Rothberg, L. J. *Science* **1995**, *267*, 1969. (d) Strukelj, M.; Miller, T. M.; Papadimitrakopoulos, F.; Sehwan, S. *J. Am. Chem. Soc*. **1995**, *117*, 11976. (e) Lee, Y.-Z.; Chen, S.-A. *Synth. Met*. **1999**, *105*, 185. (f) Burn, P. L.; Grice, A. W.; Tajbakhsh, A.; Bradley, D. D. C.; Thomas, A. C. *Adv. Mater*. **1997**, *9*, 1171. (g) Pösch, P.; Fink, R.; Thelakkat, M.; Schmidt, H.-W. *Acta Polym.* **1998**, *49*, 487. (h) Cacialli, F.; Friend, R. H.; Bouché, C.-M.; Le Barny, P.; Facoetti, H.; Soyer, F.; Robin, P. *J. Appl. Phys.* **1998**, *83*, 2343. (i) Fukuda T.; Kanbara, T.; Yamamoto, T.; Ishikawa, K.; Takezoe, H.; Fukuda, A. *Appl. Phys. Lett*. **1996**, *68*, 2346. (j) O'Brien, D.; Weaver, M. S.; Lidzey, D. G.; Bradley, D. D. C. *Appl. Phys. Lett*. **1996**, *69*, 881. (k) Jandke, M.; Strohriegl, P.; Berleb, S.; Werner, E.; Brüttig, W. *Macromolecules* **1998**, *31*, 6343.

(13) (a) Braun, D.; Heeger, A. J. *Thin Solid Films* **1992**, *216*, 96. (b) Parker, I. D. *J. Appl. Phys*. **1994**, *75*, 1656.

(14) Hoofman, R. J. O. M.; de Hass, M. P.; Siebbeles, L. D. A.; Warman, J. M. *Nature* **1998**, *392*, 54.

(15) (a) Chen, S.-A.; Lee, Y.-Z. Poly(*p*-phenylenevinylene)s Modified with 2,5-Diphenylene-1,3,4-Oxadiazole Moieties as EL Materials. Presented in the International Conference on Organic Electroluminescent Materials, September 14−17, 1996, Rochester, New York. (b) Bao, Z.; Peng, Z.; Galvin, M. E.; Chandross, E. A. *Chem. Mater.* **1998**, *10*, 1201.

(16) (a) Chung, S.-J.; Kwon, K.-Y.; Lee, S.-W.; Jin, J.-I.; Lee, C. H.; Lee, C. E.; Park, Y. *Adv. Mater.* **1998**, *10*, 1112. (b) Peng, Z.; Zhang, *J. Chem. Mater*. **1999**, *11*, 1138. (c) Meng, H.; Yu, W.-L.; Huang, W. *Macromolecules* **1999**, *32*, 8841.

(17) (a) Cacialli, F.; Li, X.-C.; Friend, R. H.; Moratti, S. C.; Holmes, A. B. *Synth. Met*. **1995**, *75*, 161. (b) Boyd, T. J.; Geerts, Y.; Lee, J.-K.; Fogg, D. E.; Lavoie, G. G.; Schrock, R. R.; Rubner, M. F. *Macromolecules* **1997**, *30*, 3553.

(18) (a) Grice, A. W.; Tajbakhsh, A.; Burn, P. L.; Bradley, D. D. C. *Adv. Mater*. **1997**, *9*, 1174. (b) Peng, Z.; Bao, Z.; Galvin, M. E. *Adv. Mater*. **1998**, *10*, 680. (c) Peng, Z.; Bao, Z.; Galvin, M. E. *Chem. Mater*. **1998**, *10*, 2086. (d) Song, S.-Y.; Jang, M. S.; Shim, H.-K.; Hwang, D.-H.; Zyung, T. *Macromolecules* **1999**, *32*, 1482. (e) Pei, Q.; Yang, Y. *Adv. Mater*. **1995**, *7*, 559. (f) Grüner, J.; Friend, R. H.; Huber, J.; Scherf, U. *Chem. Phys. Lett.* **1996**, *251*, 204. (g) Huang, W.; Meng, H.; Yu, W.-L.; Gao, J.; Heeger, A. J. *Adv. Mater*. **1998**, *10*, 593.

(19) (a) Tamoto, N.; Adachi, C.; Nagai, K. *Chem. Mater.* **1997**, *9*, 1077. (b) Antoniadis, H.; Inbasekaran, M.; Woo, E. P. *Appl. Phys. Lett.* **1998**, *73*, 3055.

(20) Wudl, F.; Srdanov, G. U.S. Patent. 5,189,136, 1993..

Scheme 1. Synthetic Route for the Present New Series of Soluble Copolymers with OXD on the Side Chain

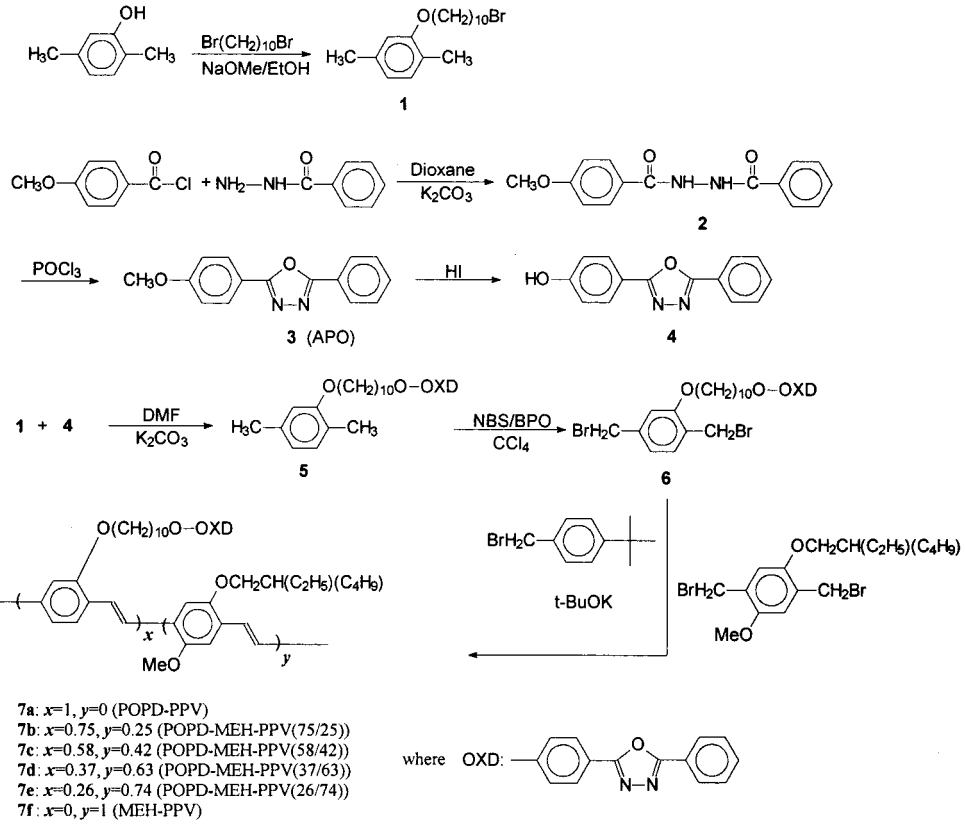

the main chains. Different from the method via Heck reaction as reported by Bao et al.[15b] (by which the maximum permissible content of comonomer with OXD in the copolymer is 50% by mole), the present copolymerization route allows an incorporation of OXD content at the full composition range, enabling a balance of electron and hole at various levels. At the optimal ratio of POPDPV to MEHPV with Ca as cathode, 37/63 by mole, the electroluminescent efficiency and brightness are significantly improved by factors of 9.4 and 30, respectively, in comparison with those of the corresponding homopolymer, MEH−PPV, based devices. It should be noted that the present work has no attempt to search for the best electron-deficient moiety. It merely intends to demonstrate the superiority of the present method over the methods of physical blending and multiplayer device structure. For the purpose of molecular design studies, no modification on the two interfaces with the electrodes has been attempted.

Experimental Section

Synthesis. The synthesis routes for the polymers used are described in Schemes 1−3. The preparations of polymers **7a**−**7f** and **13** and poly(2,5-di-decyloxy phenylene vinylene) (PdDPV) were conducted using the modified Gilch method.[21] Poly(decyloxy phenylene vinylene) (PDPV) (**12**) was prepared by the Wessling precursor.[22] The detailed synthesis procedures for the monomers and polymers are described in the Supporting Information.

Instrumentation. Various spectroscopies, near field scanning optical microscopy (NSOM),[23] elemental analysis, cyclic voltammetry (CV), gel permeation chromatography (GPC), the film thickness monitor used for the characterization of samples, and the power supply and luminance meter for measurements of device performance are also described in detail in the Supporting Information.

Device Fabrication and Characterizations. The copolymers as well as MEH−PPV and POPD−PPV so prepared were used as emitting layers. Each polymer was spin-coated on an ITO glass pretreated with UV (254 nm)/ozone from its solution in $CHCl_3$ (5 mg/mL) in air to give a thin film of about 50−100 nm thickness. On top of it, a thin layer of aluminum alone or of calcium covered with a layer of aluminum was deposited as the cathode by thermal evaporation at a pressure of 10^{-5} Torr; the active area is about 10 mm^2. The device was then transferred quickly to a vacuum cell and subjected to measurements on performance under a vacuum of about 300 mTorr. For devices with Ca, a thin layer of poly(styrene sulfonic acid) doped poly(ethylenedioxythiophene) (PEDOT−PSS) was also introduced on ITO before coating an emissive layer for comparison purposes.

Results and Discussion

A. Ultraviolet−Visible (UV−Vis) and Photoluminescent (PL) Spectroscopies. 1. Homopolymers (PDPV, POPD−PPV, MEH−PPV), and Copolymers (POPD−MEH−PPVs). Figure 1 shows the UV−vis absorption spectra of thin films of the homopolymers: PDPV (**12**), POPD−PPV (**7a**), MEH−PPV (**7f**), and copolymers, POPD−MEH−PPV of various compositions (**7b**−**7e**). Each of the corresponding PL spectra (Figure 2a) excited by the light at the absorption λ_{max} of main chains shows only one emission peak from the main chains and no emission from the oxadiazole moieties; the emission peak excited at 300 nm is the same. The characteristic values are listed in Table 1.

The absorption spectra of POPD−PPV and its copolymers each exhibit a main absorption peak at 464−500 nm contributed from conjugated main chains and an additional absorption peak at 298 nm contributed from oxadiazole moieties since the model compound, *p*-anisoyl 5-phenyl 1,3,4-oxadiazole (APO, com-

(21) Hsieh, B. R.; Yu, Y.; Forsythe, E. W.; Schaaf, G. M.; Feld, W. A. *J. Am. Chem. Soc.* **1998**, *120*, 231.

(22) (a) Liang, W. B.; Lenz, R. W.; Karasz, F. E. *J. Polym. Sci., Part A: Polym. Chem.* **1990**, *28*, 2867. (b) Shim, H. K.; Hwang, D. H.; Lee, K. S. *Makromol. Chem.* **1993**, *194*, 1115.

(23) Lee H, T.; Chuang, K. R.; Chen, S.-A.; Wei, P. K.; Hsu, J. H.; Fann, W. S. *Macromolecules* **1995**, *28*, 7645.

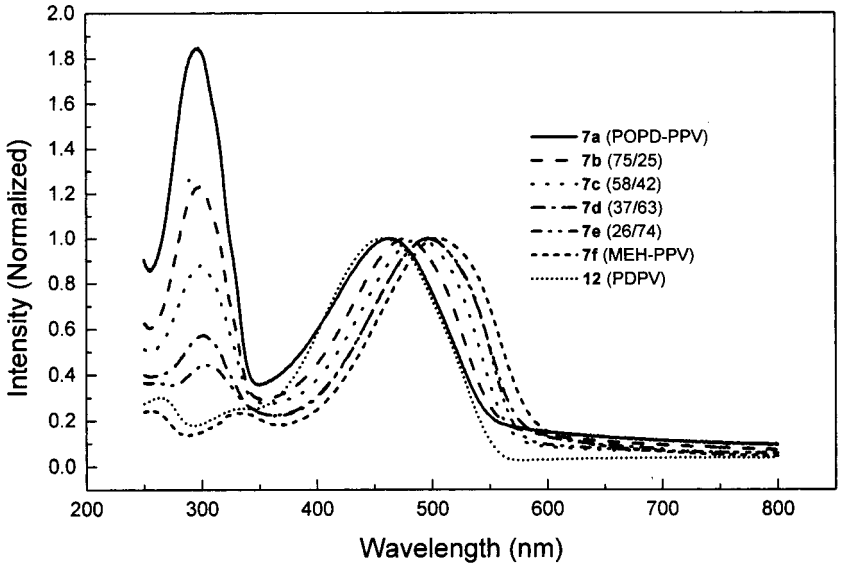

Figure 1. Absorption spectra of thin films of PDPV, POPD−PPV, MEH−PPV, and POPD−MEH−PPV copolymers.

Scheme 2. Synthetic Route for the Model Homopolymer without OXD Moiety in the Side Chain (PDPV)

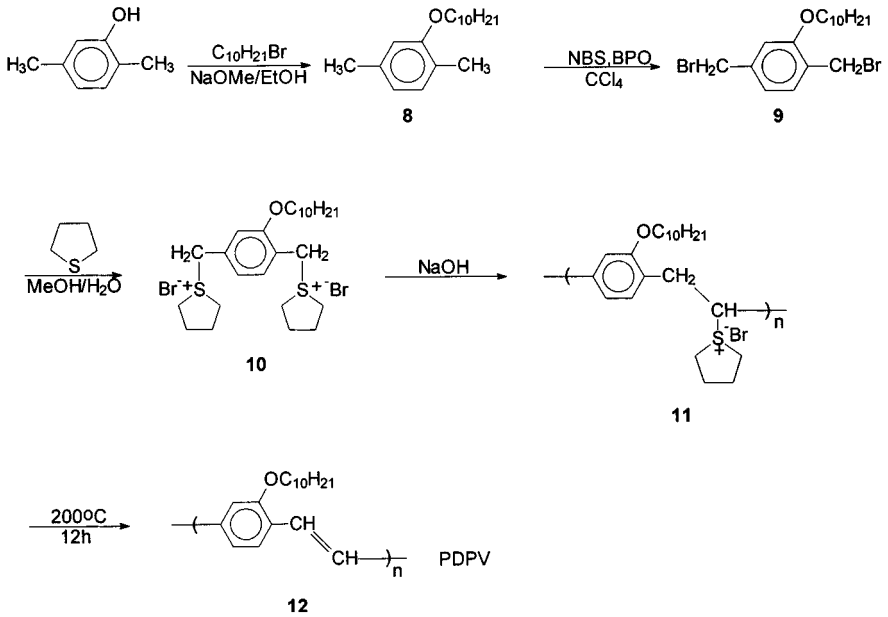

Scheme 3. Synthetic Route for the Model Copolymer without OXD Moiety in the Side Chain (DO−MEH−PPV)

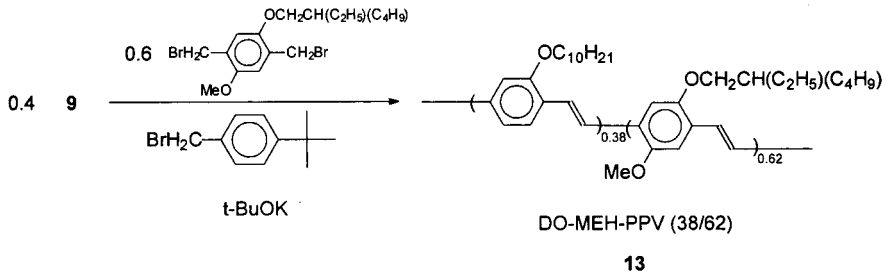

pound **3**), in toluene has a λ_{max} at 296 nm. The former peak and band gap (E_g) (Table 1) have blue-shifts as compared to those of MEH−PPV 505 nm and 2.1 eV, and extents of the shifts increase with the content of the repeat unit of polymer **7a**, POPDPV unit. The corresponding emission spectra also exhibit a similar trend of blue-shift as the content of OXD increases. Such blue-shift is not contributed from the OXD groups but is from the reduced content of electron-donating oxygen atom attached to the phenylene ring in the main chain, since the monoalkoxy-substituted PPV (POPD−PPV) has absorption $\lambda_{max} = 464$ nm and $E_g = 2.25$ eV and emission $\lambda_{max} = 549$ nm, which are very close to those of its parent polymer (without OXD units) PDPV (absorption $\lambda_{max} = 458$ nm and $E_g = 2.22$ eV and emission $\lambda_{max} = 555$ nm). In the emission spectra of POPD−PPV and the copolymers excited at 300 nm, the absence of the emission peak at about 350−380 nm from OXD group in its corresponding compound APO (**3**) (see the emission

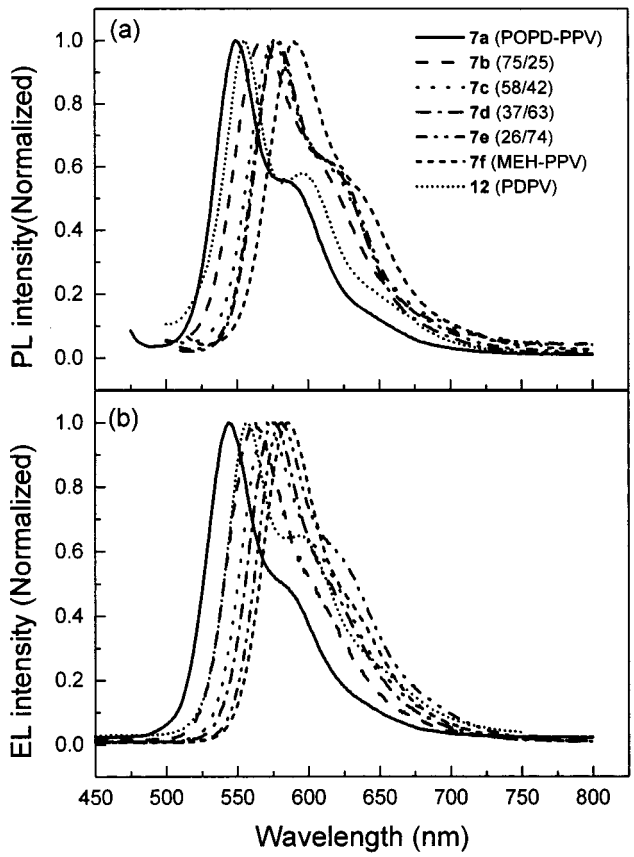

Figure 2. Photoluminescence (a) and electroluminescence (b) spectra of thin films of PDPV, POPD−PPV, MEH−PPV, and POPD−MEH−PPV copolymers. The former were measured under ambient condition, and excited by the light of absorption maximum of conjugated main chain and the latter from the device with the same materials, ITO/polymer/Ca/Al.

spectrum of APO in poly(methyl methacrylate) in Figure 5) would indicate the occurrence of nonradiative energy transfer.

The photoluminescence excitation spectra (PLE) (shown in Figure 3) of PDPV, POPD−PPV, MEH−PPV, and POPD−MEH−PPVs as thin solid films were monitored at the λ_{max} of the emission spectrum of each polymer. The PLE of PDPV is similar to the absorption spectrum, while that of POPD−PPV monitored at 549 nm shows a broad peak covering 275−345 nm (contributed from the OXD moieties), which is only about 7% of the total emission intensity and much weaker than the absorption intensity of the OXD relative to that of the main chains. This would indicate that the efficiency of energy transfer from OXD to the main chains is low and its contribution to the emission intensity from the main chain is insignificant. As the content of the comonomer with OXD, POPDPV unit, decreases, the contribution from energy transfer decreases accordingly.

2. Blends of DO−MEH−PPV (13) with APO (3) and of POPD−PPV (7a) with MEH−PPV (7f). To explore the interaction between the conjugated main chain and heterocyclic side groups in the OXD-modified PPVs, DO−MEH−PPV (38/62) (polymer **13**) was synthesized, which is soluble and has the same chemical composition as polymer **7d** but without the electron-withdrawing group, OXD. Except for the absorption of OXD moiety, the UV−vis spectra and *E*g of the two statistical copolymers are nearly identical, again indicating no contribution from OXD to the absorption spectrum of the main chain. Polymer **13** is blended with APO at the mole ratio 100/37 in chloroform to yield a homogeneous solution (5 mg/mL) and as a solid film by casting from the solution to simulate polymer **7d**. The normalized UV−vis and PL spectra (excited by the light 300 nm) of the blend in the dilute chloroform solution (0.005 mg/mL) and as a thin solid film are shown in Figures 4 and 5, respectively, in which the spectra of polymer **7d** are also depicted for comparison.

As shown in Figure 4, the absorption spectra of polymer **7d** in solution and as a solid film contributed from the conjugated main chains are very close to those of its corresponding blend in the same states, respectively. For OXD moieties in the blend and polymer **7d**, their absorption maxima are also close in both states, but their intensities relative to those of the main chains are likely dependent on the micro-environments. For the blend in the solution and as solid film, the absorption intensities at 300 nm are quite different; the contribution of each OXD group in the former is much higher than that in the latter, indicating a greater isolation of APO molecules in the former. For polymer **7d** in both states, the absorption intensities at 300 nm are the same, even though the OXD moieties in the solution are surrounded with chloroform molecules. This would indicate that the extent of interaction between OXD and the main chain is nearly the same in both states and is not disturbed by the surrounding chloroform molecules in the solution. Thus, their interaction must be intrachain in nature.

For the emission spectra, the roles of OXD are dramatically different from those in the absorption spectra. As shown in Figure 5, for the blend in solution, the emission intensity from APO is overwhelmingly higher than that from the conjugated main chains, which appears only as a very small bump. This is because APO has a much higher quantum efficiency than polymer **13**. However, for the blend as solid film, the emission intensity from APO is highly suppressed and much smaller than that from polymer **13,** while its emission spectrum is similar to that of its blend with poly(methyl methacrylate) (PMMA) having the same weight ratio as the blend of APO/polymer **13**. In contrast to the blend system, the copolymer POPD−MEH−PPV (37/63) (polymer **7d**) has weak emission contributed from the OXD side group both in the solution and as solid film. The result can be explained by Förster energy transfer[24] from OXD group to the conjugated main chain. The energy-transfer efficiency is related to the overlap of the absorption spectrum of the conjugated main chain with the emission spectrum of OXD moieties, and the distance of OXD moieties with conjugated main chains. For the blend in solution, no energy transfer occurs because APO molecules are moving around and have little chance to stay close enough to the conjugated main chains of polymer **13** to allow energy transfer. For the blend as solid film, these two species could come closer. Since the spectra overlapping is not sufficient and the phase separation is obvious, the extent of energy transfer is limited, and the emissions from APO can still be detected. For polymer **7d** in the solution and as solid film, the OXD moiety is bonded to the main chain by a favorable distance to allow an intramolecular energy transfer.

The other way to simulate the copolymer **7d** is by blending POPD−PPV (**7a**) with MEH−PPV (**7f**) at the mole ratio of their repeat units at 37/63. The absorption and emission spectra of the copolymer and blend as solid films on quartz are shown in Figure 6. As can be seen, both spectra of these two materials are very close except that polymer **7d** shows a more obvious shoulder at about 640 nm in the emission spectrum, which is the characteristic of the monosubstituted PPVs, POPD−PPV, or PDPV (Figure 2). The presence of the single peak from the main chains in the absorption and emission spectra of the blend

(24) Meer, B. W. v. d.; Coker, G.; Chen, S.-Y. S. *Resonance Energy Transfer: Theory and Data*; VCH Publishers: New York, 1994.

Table 1. Compositions of Copolymers (**7b**−**7e**), Absorption and PL Maxima and E_g, IP, and EA Parameters of PDPV and Polymers **7a**−**7f**

polymers	**7a**	**7b**	**7c**	**7d**	**7e**	**7f**	PDPV
feed ratio (6a:6b)	100:0	80:20	60:40	40:60	25:75	0:100	-
composition (x:y)[a]	-	75:25	58:42	37:63	26:74	-	-
$\overline{M_w}$ (10^4)[b]	-	25	39	35	11	24	-
polydispersity (PD)[c]	-	1.7	3	3.2	4.1	4.1	-
UV−vis λ_{max} (nm)[d]	464	479	490	496	498	505	458
PL λ_{max} (nm)	549	567	576	578	578	590	555
E_g[e] (eV)	2.25	2.2	2.16	2.14	2.12	2.1	2.22
IP[f] (eV)	5.44	5.3	5.03	5	4.97	4.95	5.11
EA[g] (eV)	2.95	2.92	2.86	2.83	2.86[i]	2.85	-
EA[h] (eV)	3.19	3.1	2.87	2.86	2.85	2.85	2.89

[a] Determined from the ratios of protons on OXD moiety and on benzene ring of MEHPV in ^{1}H NMR. [b] $\overline{M_w}$: weight average molecular weight. [c] PD = $\overline{M_w}/\overline{M_n}$, where $\overline{M_n}$ $\langle mx \rangle$ is number average molecular weight. [d] Absorption maximum of conjugated main chain. [e] Determined from the edge of the red end of absorption spectrum. [f] Determined from the onset of the oxidation curve of cyclic voltammetry measurement. [g] Determined from the onset of the reductive curve of cyclic voltammetry measurement. [h] Calculated from the equation EA = IP − E_g. [i] The reduction curve of CV measurement of **7e** does not appear in Figure 10b in order to make the other curves easy to be distinguished.

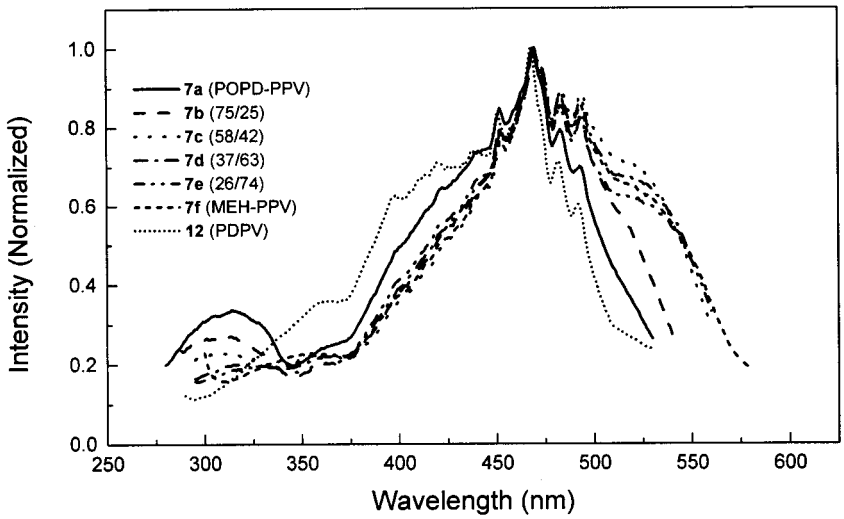

Figure 3. Photoluminescence excitation spectra of PDPV, POPD−PPV, MEH−PPV, and POPD−MEH−PPV copolymers, monitored at the PL emission peak of each polymer.

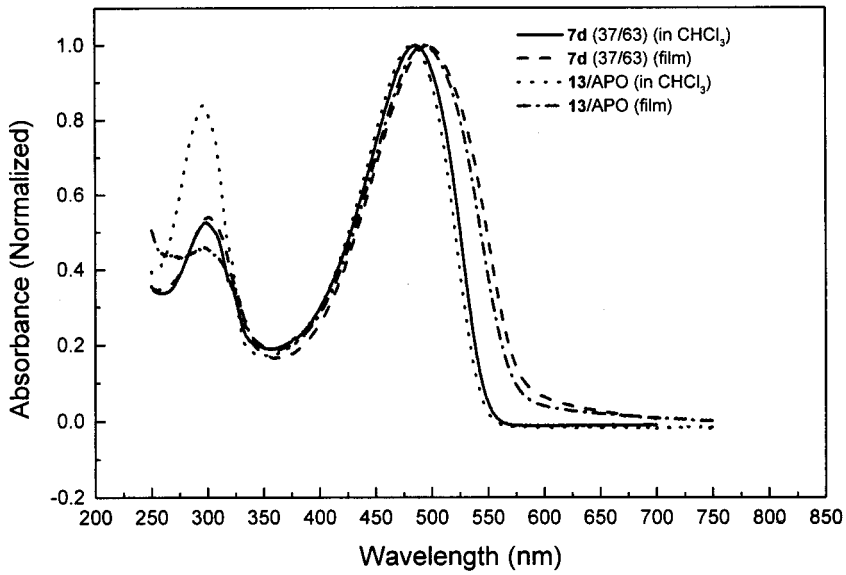

Figure 4. Absorption spectra of polymer **7d** (POPD−MEH−PPV (37/63)) and blend of polymer **13**/APO (100/37 by mole) in $CHCl_3$ solution and as thin solid films.

cannot be used to infer that the two components are miscible, since the calculated absorption and emission spectra based on the molar additivity rule also give a single peak at the same wavelength (Figure 6). Actually, the blend is still immiscible in submicrometer scale, and the two components still retain some of their own characteristics which will be resolved in the next section on the morphological observation.

B. Morphology and Chain Conformation. Further efforts being taken to explore the interaction between OXD and conjugated main chain in the copolymers are to observe the extent

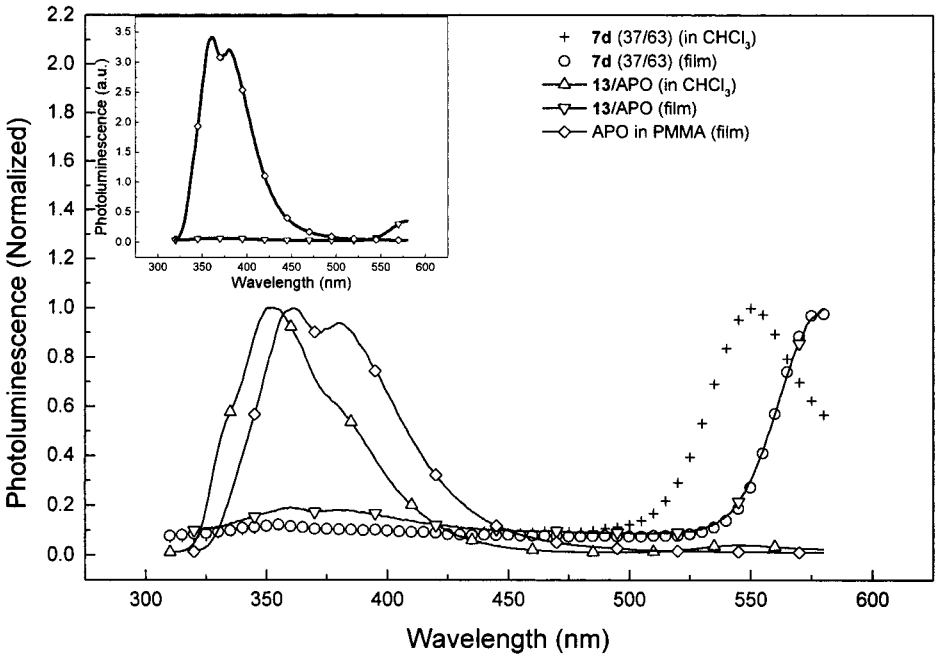

Figure 5. Photoluminescence spectra of polymer **7d** (POPD−MEH−PPV (37/63)) and polymer **13**/APO blend (100/37 by mole) in $CHCl_3$ solution and as thin solid film, poly(methyl methacrylate) (PMMA)/APO blend as thin solid film excited by light at 300 nm. The inset shows the relative non-normalized curves of thin films of the blend polymer **13**/APO and PMMA/APO prepared under the same fabrication condition.

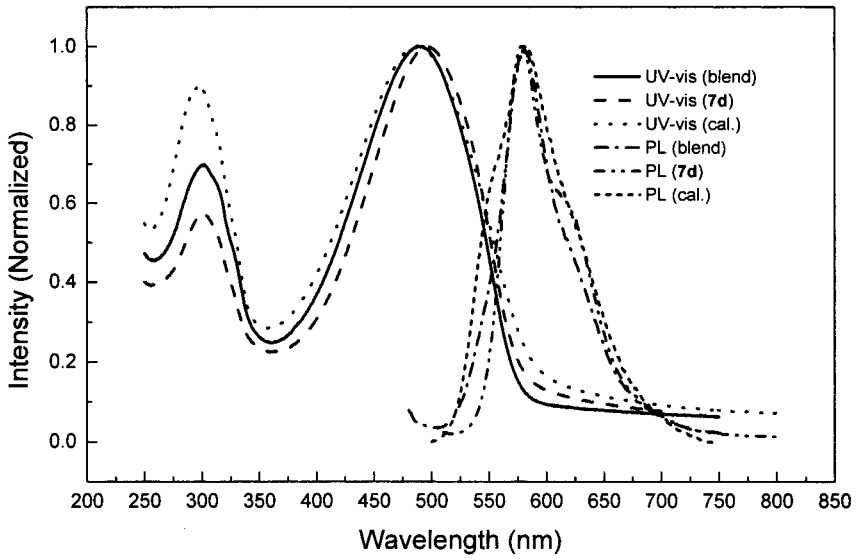

Figure 6. Absorption and PL spectra of the blend of POPD−PPV (**7a**) with MEH−PPV (37/73 by mole of their repeat units) and polymer **7d** (POPD−MEH−PPV (37/63) as thin films on quartz and those of the same blend calculated on the basis of the spectra of the individual homopolymers by use of the molar additivity rule.

of dispersion of the former in the latter relative to those in the blends of POPD−PPV with MEH−PPV by use of near field scanning optical microscopy (NSOM) and wide-angle X-ray diffraction (WAXD) and of DO−MEH−PPV (**13**) with APO using optical microscopy. The morphology of MEHPPV, the present copolymers, and the two physical blends can be represented schematically as shown in Figure 7 as to be revealed below.

Figure 8 shows the topographic and NSOM images in transmission mode on the same location of the thin films about 100 nm thick of polymer **7d** and the blend of POPD−PPV with MEH−PPV (mole ratio 37/73) coated on glass substrates using 0.5 mW green He−Ne laser source of 543.5 nm with a beam diameter of 100 nm. This light source is able to distinguish the two components in the blend since the ratio of the absorbance of the latter to that of the former is about 3.4 (Figure 1). The dark and bright regions in the NSOM image would indicate a MEH−PPV-rich and a POPD−PPV-rich regions, respectively. For the topographical image, the brighter region indicates a region with larger thickness. For polymer **7d**, both the topographic and NSOM images (Figure 8a) are as featureless as that for MEH−PPV, indicating a film with smooth surface and a random distribution of the two repeat units in the copolymer; its morphology can be represented schematically by Figure 7b. For the blend (Figure 8b), the topographical image shows a more uneven surface; the majority of the domains are bright and thus thicker with the size about 1 μm. Its NSOM image shows a different texture. The domain size of the dark region (MEH−PPV-rich) is about 0.1−1 μm, while that of the bright region (POPD−PPV-rich) is about 0.5−1 μm. Both the dark and bright regions form interwoven networks and have no sharp boundary between them, which indicates a phase-separation structure with some extent of intermixing as shown schematically in Figure

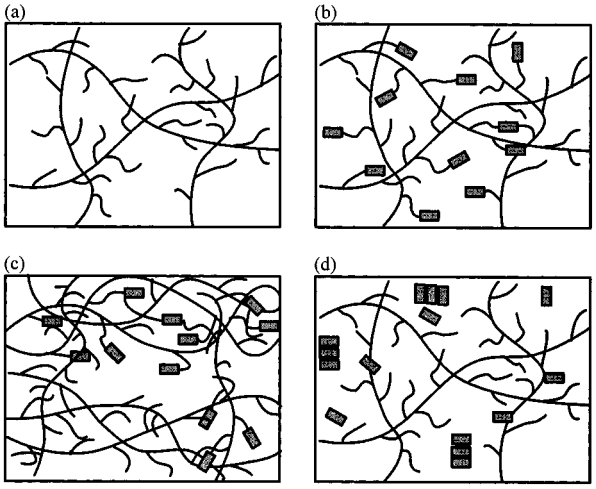

Figure 7. The schematic morphology of (a) MEH−PPV, (b) the present copolymers, (c) blend of MEH−PPV with POPD−PPV (**7a**), and (d) blend of DO−MEH−PPV (**13**) with APO. The blocks represent the OXD moieties.

7c. Since the domain sizes of both dark and bright regions are greater than the thickness of emission layer (100 nm) in the device, each region forms an independent pathway for charge transport. Thus, the emission color is expected to be dependent on the applied bias as it actually occurs as to be revealed in the later section.

For the blend of DO−MEH−PPV (**13**) with APO, phase separation also occurs. A domain size of about a few to 10 μm for APO phase was observed from its thin film (about 100 nm thick) on a glass plate under an optical microscope. Its film morphology is not convenient to be examined using NSOM due to the large domain size and can be schematically represented by Figure 7d.

WAXD (Figure 9 a) for the copolymers in the entire composition range, POPD−MEH−PPVs, show that the copolymers are amorphous and have no side chain alignment, while the two corresponding homopolymers are also essentially amorphous but with very small extent of side chain alignment as reflected in the presence of a small hump in the 2θ range 3°−7°. The nearly amorphous structure of the homopolymers (Figure 7a) originates from the two highly asymmetric substituents, the methoxy and 2-methoxy 5-(2′-ethoxyhexyloxy) for MEH−PPV and from the monosubstitution with the long side chain, decyloxy for PDPV (Figure 9b). For symmetrical di-substitution such as poly(2,5-di-decyloxy phenylene vinylene) (PdDPV), the side chain alignment is very pronounced as reflected in the presence of an intense and sharp diffraction peak at 4° (Figure 9b). The copolymerization of the monosubstituted PV with asymmetrically disubstituted PV further makes the side chain alignment even more difficult and thus leads to the highly amorphous structure.

This observation together with the occurrence of energy transfer from the OXD-moiety to the conjugated main chain as revealed in the above section would strongly indicate that they mixed well, which then allows the OXD moiety to act efficiently as a bridge during the interchain electron transport.

C. Cyclic voltammetry (CV). CV is a well-known electrochemical method for exploration of relative ionization and reduction potentials. The CV measurements of the present copolymers in Figure 10 a show that the oxidation onsets of the copolymers **7c** (58/42), **7d** (37/63), and **7e** (25/75) contributed from the conjugated main chain are respectively higher only by 0.08, 0.05, and 0.02 eV than that of **7f** (MEH−PPV), while those of **7a** (100/0) and **7b** (75/25) are much higher than **7f** by 0.49 and 0.35 eV, respectively. (The CV curve for **7e** does not appear in the figure in order to make the other curves easy to be distinguished.) The oxidation peak for OXD moiety should be quite high and was not accessible in the scan range. The higher oxidation onsets and irreversible redox processes of **7a** and **7b** are due to higher electrical resistance imparted by the high content of OXD, which covers major parts of the electrode surface, causing a need of an additional electric field to overcome the anion diffusion barrier. This phenomenon also appears in the device performance. The turn-on electric field shifts significantly to higher electric field for the devices with Ca and Al as cathodes (see the inset of Figure 10a). Therefore, for **7a** and **7b**, the ionization potential (IP) values determined this way cannot be considered as real ionization potential of the bulk polymer, but provide useful information for exploring the performance of the device. For the lower OXD-containing copolymers, **7c**, **7d**, and **7e**, the redox reversibility is quite good, and the oxidation onset can be used for calculating their IP values. The IP values (determined from the oxidation onsets versus the ferrocene/ferrocenium system,[25] in which the IP of ferrocene is 4.8 eV, and the equation: $IP = 4.8 + V_{onset}$ (versus Fc/Fc^+)) of copolymers **7a**−**7e** and MEH−PPV (**7f**) are listed in Table 1. The potential of Fc/Fc^+ was measured as 0.52 V versus Ag/AgCl (the reference electrode used in this work); this value can be used to convert the experimental potentials versus Ag/AgCl to those versus Fc/Fc^+ for calculating IP. The band diagram (Figure 11) constructed from the IP and E_g values (listed in Table 1) indicates that both EA ($= IP - E_g$) and IP of the copolymers with POPDPV content below 60% by mole increase only slightly with the OXD content in the copolymers by about 0−0.02 eV and 0.02 −0.08 eV, respectively, and the extent of increase of IP is higher than that of EA, implying that the barrier for electron injection decreases but that for hole injection increases.

Since the reduction scan of our polymers using propylene carbonate as the solvent is not accessible, we choose the less polar solvent, pentanenitrile, to run the n-doping. Although acetonitrile has been used as a solvent in the oxidation and reduction scans of MEH−PPV by the others,[26] it was found to be not applicable to the present polymers with OXD. When the scan voltage is limited above −1.8 V versus Ag/AgCl, the CV measurements in Figure 10b for the reduction potentials of **7f** (MEH−PPV) and the polymers **7a**−**d** all show a pair of reversible peaks. As in the oxidation scan, the variation of reduction potential for the polymers with different OXD content is very low, only by about 0.05 eV except for that of the homopolymer, **7a**, which can be attributed to its reduced conductivity at the interface with the electrode imparted by the coverage of OXD groups. Thus, these reduction potentials must be originatingfrom the main chains, and the onsets of reduction process can be used for calculating EA of the materials. The measured EA ($EA = 4.8 + V_{onset}$ vs Fc/Fc^+)[25] values are quite close to the calculated values from IP and E_g and are listed in Table 1. For the reduction scan of OXD groups, a model compound APO is used and its reduction potential was measured as −2.07 V versus Ag/AgCl (the inset of Figure 10c). For the OXD moieties in the polymers, we extended the scan range further down to −2.3 V versus Ag/AgCl and found two reduction peaks and a small shoulder between them as shown in Figure 10c. The first peak

(25) (a) Gritzner, G.; Kuta, J. *Pure Appl. Chem.* **1984**, *56*, 461. (b) Bredas, J. L.; Silbey, R.; Boudreaux, D. S.; Chance, P. R. *J. Am. Chem. Soc.* **1983**, *105*, 6555.

(26) Richter, M. M.; Fan, F.-R. F.; Klavetter, F.; Heeger, A. J.; Bard, A. J. *Chem. Phys. Lett.* **1994**, *226*, 115.

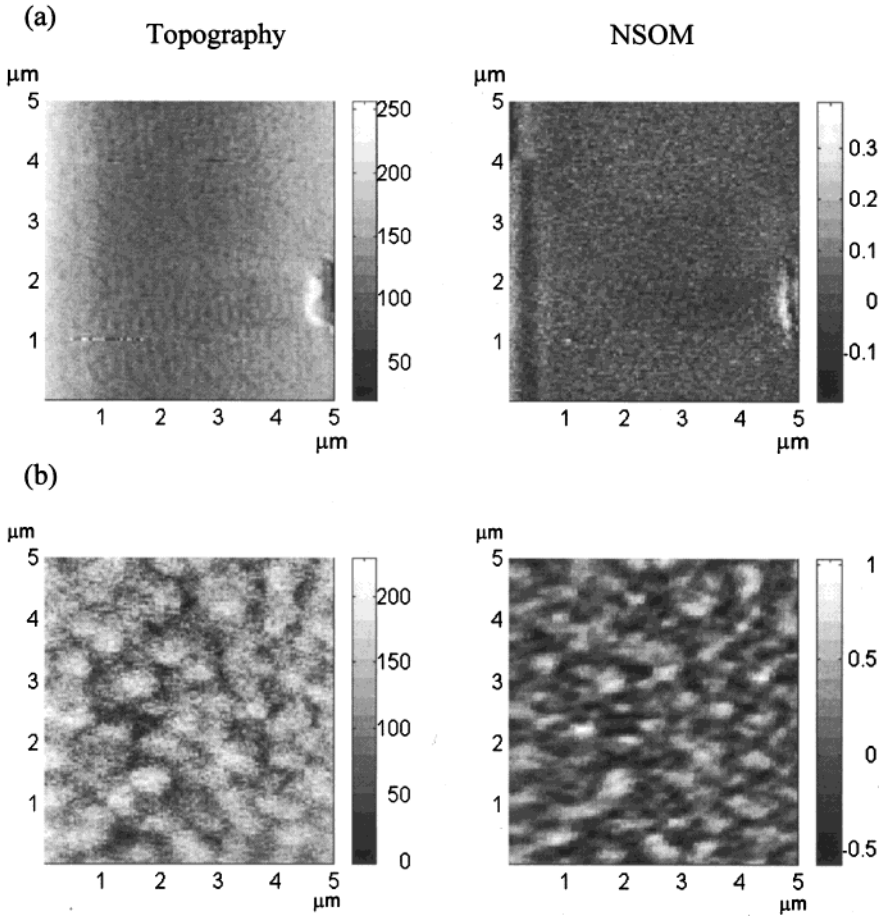

Figure 8. Topographic (height ruggedness scale unit: Å) and near field scanning optical microscopy images (transmission mode with arbitrary intensity scale) of thin films of (a) POPD−MEH−PPV(37/63) (**7d)** and (b) blend of POPD−PPV(**7a**)/MEH−PPV (37/73).

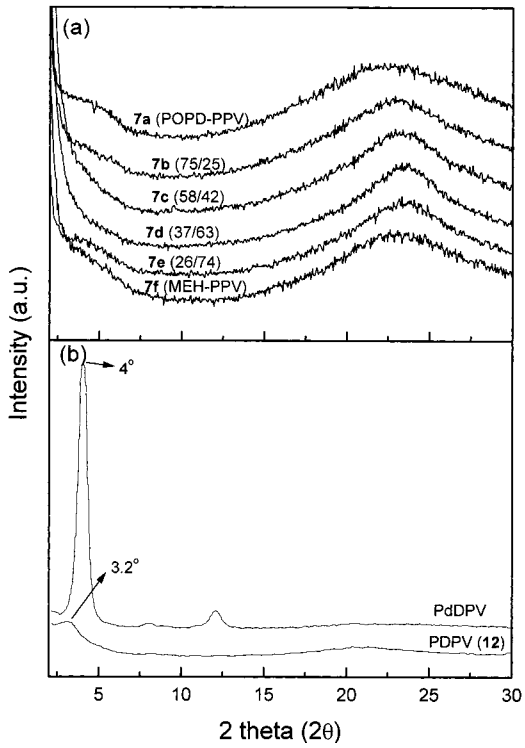

Figure 9. Wide-angle X-ray diffraction patterns of (a) POPD−PPV (**7a**), MEH−PPV and POPD−MEH−PPVs; (b) PdDPV and PDPV (**12**).

is similar to that in the narrow scan in Figure 10b and can be assigned again to the main chain. The second peak is almost at the same position as for APO and the peak height relative to the first increases with OXD content in the polymers; thus, it can be assigned to the OXD group. The reduction current for OXD is quite high as compared to that for the main chain, suggesting that the OXD group is very capable of accepting electrons and, as expected, is an efficient electron-transport site. The shoulder between these two peaks could originate from the main chain, since the second reduction peak of MEHPPV appears close to this shoulder. In the reverse scan, the polymer starts to dissolve into the supporting electrolyte, and the current for undoping becomes small. The origin of the second reduction peak of MEH−PPV is not known at the present time. Further investigation into this phenomenon is necessary.

The CV results would indicate that both the side chain and main chain do retain their own electronic characteristics in the copolymer films. Thus, the role of OXD for significant improvement in electron transport in the bulk and electron injection at the electrode surface can be expected. Similar results for other electron-deficient moieties on the side chain can also be expected. This approach is better than that of adding an electron-transport layer, such as the OXD compound, 2-(4-biphenylyl)-5-(4-*tert*-butyl-butylphenyl)-1,3,4-oxadiazole (PBD),[27] with which the barriers for electron injection increase significantly by 0.49 eV (Figure 11). The PBD seems to act as a hole-blocking layer rather than an electron-transporting layer.

D. Device characteristics. 1. Homopolymers (PDPV, POPD−PPV, MEH−PPV) and Copolymers (POPD−MEH−PPVs) as Emitting Layer. The electroluminescent (EL) spectra of the devices, ITO/polymer/Ca and Al, (Figure 2b) are very

(27) Janietz, S.; Wedel, A. *Adv. Mater*. **1997**, *9*, 403.

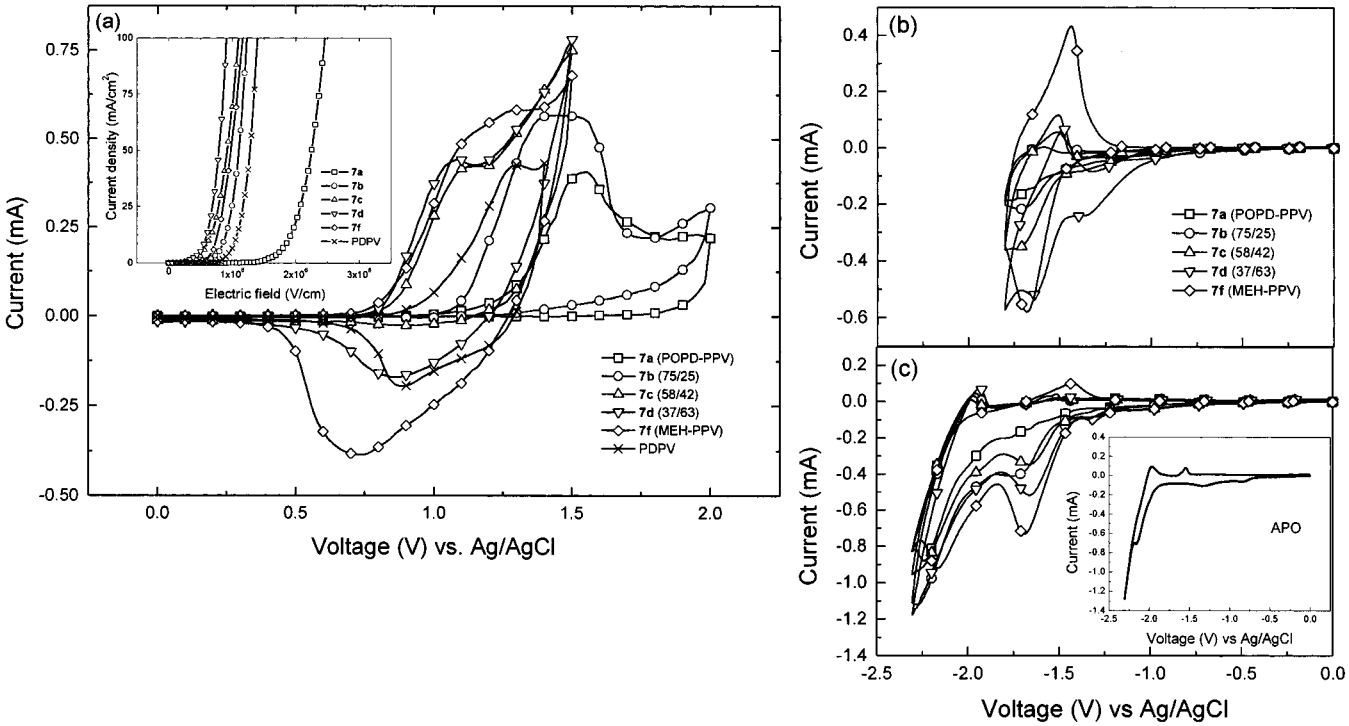

Figure 10. Cyclic voltammograms of the PPV derivatives on ITO substrate (a) in 0.1 M Bu_4NClO_4 in dry propylene carbonate, (b) and (c) in 0.5 M Bu_4NClO_4 in pentanenitrile. The inset in (a) shows the characteristics of current density versus electric field of PLEDs with the PPV derivatives as emissive material and Ca as the cathode. The inset in (c) shows the reduction scan of APO in the supporting electrolyte solution with the same measurement condition as for (b) and (c).

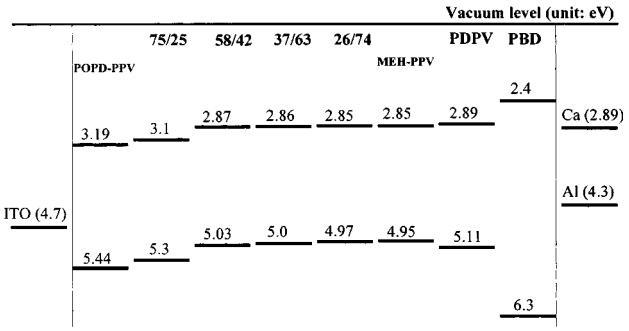

Figure 11. Band diagram of PDPV (**12**), POPD−PPV (**7a**), POPD−MEH−PPVs, MEH−PPV and PBD with the work functions of ITO, Al, and Ca.

close to the PL spectra of the corresponding polymers (Figure 2a). The light emitting from the devices originates from the main chain of the emitting polymers, while OXD groups in the polymers give no contribution to the light emission. The current density−electric field ($J-E$) characteristic curves and the dependence of luminance on injected current of the single layer devices are shown in Figures 12 and 13, respectively. Their characteristic values: the maximum luminous efficiencies (LE_{max}, cd/A), the maximum external quantum efficiencies[28] which account for the difference of spectral response (η_{max}, %), the turn-on electric field (E_{to}, MV/cm) at 5 mA/cm^2, and the conductivity (σ, S/cm) of the devices at the linear region of $J-E$ plots are listed in Table 2.

A comparison of the performance of the devices of the homopolymer, POPD−PPV (**7a**), with that of MEH−PPV shows that η_{max} of the former are higher than those of the latter by the factors 1.5 (Ca) and 12 (Al) but E_{to} of the formers are higher by the factors 2.6 (Ca) and 2.1 (Al). Further comparison with that of PDPV (polymer **12**) exhibits that its η_{max} are also improved by the factors 1.2 (Ca) and 15 (Al) but its E_{to} increases

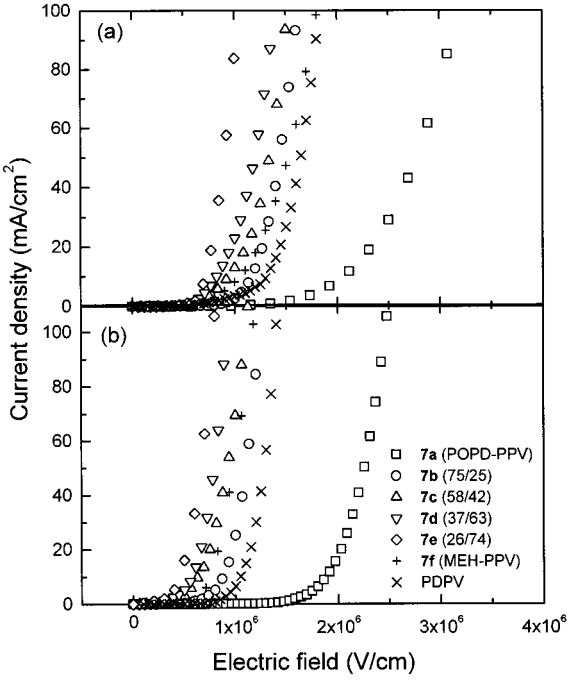

Figure 12. Current density−electric field characteristics for the devices of PPV derivatives with Al (a) and Ca (b) as the cathode.

by the factor 1.8 (Ca) and 1.7 (Al). The E_{to} increase by a factor of about 2 after the incorporation of OXD is because the hole-blocking effect is dominant over the electron injection effect.

(28) (a) Wakimoto T. In *Organic Electroluminescent Materials and Devices*; Miyata, S., Nalwa, H. S., Eds.; Gordon and Breach Publishers: 1997; p 294. (b) Greenham, N. C.; Friend, R. H.; Bradley, D. D. C. *Adv. Mater*. **1994**, *6*, 491. (c) Wilson, J., Hawkes, J., Eds.; *Optoelectronics: An Introduction*, 3rd ed.; Prentice Hall: Europe 1998; p 157. (d) See also detailed calculation method in the Supporting Information.

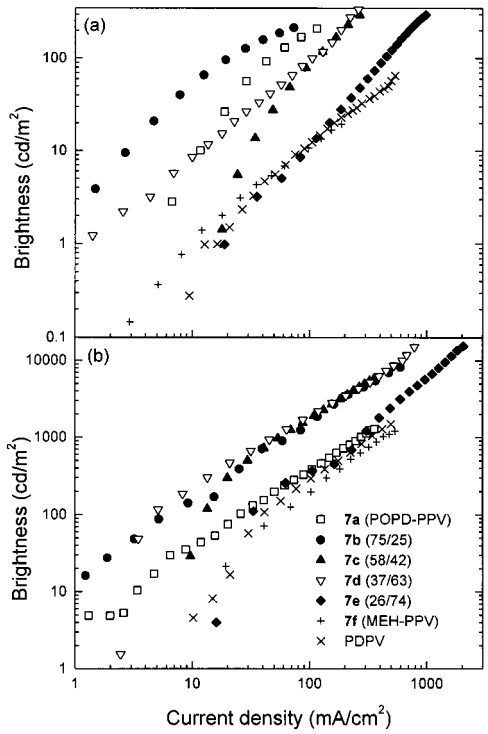

Figure 13. Brightness−current density characteristics for the devices of PPV derivatives with Al (a) and Ca (b) as the cathode.

Thus, the increase in η_{max} primarily results from the hole blocking effect of OXD.

As MEH−PV units are incorporated to form the copolymers, the performance is improved, and there is an optimum copolymer composition. The compositions where LE_{max} and η_{max} are the highest are 37/63 (Ca) and 75/25 (Al), at which the LE_{max} are improved by the factors 9.5 and 43.3 and η_{max} by 8.4 and 30, and E_{to} are reduced by 28 and 24%, respectively as compared with those of MEH−PPV. The device with Ca can reach a brightness of 15000 cd/m^2 at 1.5 MV/cm (or 15 V/100 nm), about 30 times brighter than that of the device with MEH−PPV (at the same electric field) fabricated under the same condition.

It can be expected that, if the exposure to air during the fabrication of the device is avoided, further improvement in quantum efficiency can be made. For the emitting PPV derivatives with electron-deficient moieties on the side chains and main chains reported by the others, the improvement of η_{ext} is not pronounced. For the devices with Ca, no result or poor performance was obtained; however, those with Al, the η_{ext} values, 0.02−0.15% (main chain)[18] and 0.02−0.04% (side chain),[15,16] are comparable with those of ours (0.02−0.3%).

For the devices with Ca, after the use of poly(ethylenedioxythiophene) doped with polystyrene sulfonic acid (PEDOT−PSS) from Bayer Co. as hole-transport layer, the E_{to} is further reduced, and the devices are more stable during the operation, but the improvement of η_{max} is not obvious for the low E_{to} devices with POPD−MEH−PPVs. However, the introduction of PEDOT−PSS significantly improves the efficiency and lowers the turn-on voltage of the devices with the homopolymers, POPD−PPV and MEH−PPV.

The incorporation of the co-repeat unit, POPD−PV, does lead to a balance in hole- and electron injections as can be observed from the conductivity results listed in Table 2, determined from the linear region of the $J-E$ curves.[29] The conductivity is defined as: $\sigma = J/E = q(n^+\mu^+ + n^-\mu^-)$ where q is the charge of electron or hole, n and μ are number and mobility of the charge carrier, respectively, and the superscripts "+" and "−" donate hole and electron, respectively. Thus, the conductivity value reflects the total charge flux. As the OXD group is incorporated into each repeat unit of PDPV (**7a**) to yield POPD−PPV (**12**), the conductivity determined from the device with Ca decreases from 4.09×10^{-7} S/cm to 2.29×10^{-7} S/cm, indicating that the hole-blocking effect by the OXD group dominates over its electron-transporting effect. The same situation also appears for the device with Al. As POPD−PV units are incorporated with MEH−PV units to give the copolymers **7b**−**7e**, the charge flux increases for the devices with both Ca and Al despite of the hole-blocking effect by the OXD moiety. This would indicate that the OXD moiety does provide an increase in electron flux. For the device with Ca, the total flux has a maximum at the copolymer composition 37/63 (**7d**). A maximum flux is also observed for the device with Al, but it is located at the copolymer composition 26/74 (**7e**), not the same composition as for the LE_{max} and η_{max} 75/25 (**7b**)**.** It seems that some other factors might also be involved in the performance, such as separation of electron/hole pair by the OXD moieties. The optimum copolymer composition for η_{max} of the device with Ca requires 37 mol % of OXD, lower than that with Al, 75 mol %. This is due to the lower work function of Ca than that of Al by 1.4 eV, causing the barrier for electron injection to be low and thus requiring less OXD moiety to provide a balance of charge injections.

For MEH−PPV, the intrachain mobility of the electron is found to be higher than that of the hole[13] as determined from the dilute solution in which the single chain state exists. However, the mobility of holes across the solid film is higher than that of electrons, since electrons can be easily trapped during the interchain transport.[15] Thus, the introduction of electron-deficient OXD moieties could result in a reduction of trapped electrons during the interchain transport.

2. Blends of DO−MEH−PPV (13) with APO and POPD−PPV with MEH−PPV as Emitting Layer. One way to simulate polymer **7d** is to blend DO−MEH−PPV with APO. Both the devices ITO/polymer **13**/Ca/Al and ITO/blend/Ca/Al under the forward bias show identical EL spectra, indicating that the emission is mainly from the 0−0 (singlet) transition of polymer **13**. The latter device has the E_{to} about 5.1 V/100 nm, comparable with that of the former (5.6 V/100 nm), but the maximum brightness 311 cd/m^2 and LE_{max} 0.18 cd/A are lower than those of the former (1620 cd/m^2 and 0.32 cd/A). On examination of the devices under the optical microscope, the emissive active area of the blend device shows the presence of spots, resulting from a phase separation and recrystallization of APO.[8d] Thus, the addition of APO to polymer **13** does not provide any improvement in quantum efficiency. In fact, it causes a deterioration of the device performance, and its performance is very poor compared to that of the device with polymer **7d**.

Another way to simulate polymer **7d** is to blend POPD−PPV with MEH−PPV at the mole ratio 37/63 based on their repeat units. The device with this blend and Ca has the E_{to} 9.5 V/100 nm (in between those of the devices with the two homopolymers), the maximum brightness 615 cd/m^2 at 17 V, and LE_{max} 0.5 cd/A, which are much poorer than those of polymer **7d**. The EL emission spectra are dependent on the applied voltage as shown in Figure 14. At the turn-on voltage, the EL spectrum is the same as that of MEHPPV. As the voltage increases, the intensity of the spectrum at the lower-wavelength

(29) Fang, Y.; Chen, S.-A.; Chu, M. L. *Synth. Met.* **1992**, *52*, 261.

Table 2. Device Characteristics of PDPV, POPD−PPV, MEH−PPV, POPD−MEH−PPVs, DO−MEH−PPV, and Blends

	LE_{max}, cd/A ($\eta_{max,\%}$)[a] (E_{to}, MV/cm)[b](conductivity σ, 10^{-7} S/cm)[c]		
polymer	Ca	Ca (with PEDOT−PSS)	Al
7a (POPD−PPV)	0.46(0.13)(1.75)(2.29)	1.3(0.37)(1.20)(3.58)	0.21(0.06)(1.88)(1.26)
7b (75/25)	1.79(0.54)(0.79)(3.88)	1.92(0.57)(0.48)(3.96)	0.52(0.15)(1.10)(2.64)
7c (58/42)	1.8(0.60)(0.55)(2.73)	1.68(0.56)(0.45)(4.03)	0.11(0.04)(0.81)(2.82)
7d (37/63)	2.27(0.76)(0.49)(4.42)	1.71(0.57)(0.42)(3.70)	0.13(0.04)(0.72)(2.33)
7e (26/74)	0.76(0.29)(0.39)(3.62)	0.84(0.32)(0.36)(5.47)	0.03(0.012)(0.66)(3.4)
7f (MEH−PPV)	0.24(0.09)(0.68)(2.63)	0.8(0.30)(0.59)(3.99)	0.012(0.005)(0.89)(1.58)
PDPV (**12**)	0.31(0.11)(0.96)(4.09)	- -	0.012(0.004)(1.10)(2.58)
DO−MEH−PPV(**13**)	0.34(0.13)(0.56)(3.50)	- -	- -
13/APO (100/37)	0.18(0.07)(0.51)(3.97)	- -	- -
7a/**7f** (37/63)	0.5(0.12)(0.95)(2.27)	- -	- -

[a] Calculated from the LE_{max} taking the spectral response factor into account.[28] [b] E_{to}: turn-on electric field at 5 mA/cm^2, the unit MV/cm is equivalent to 10 V/100 nm. [c] Slope of linear fitting for the current density at 40−100 mA/cm^2 of each device.

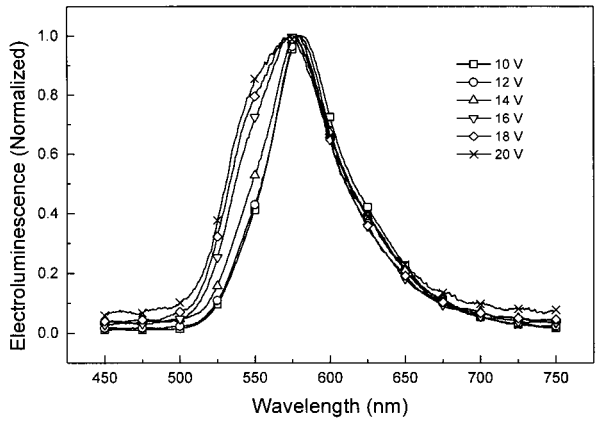

Figure 14. Electroluminescent spectra of ITO/POPD−PPV (**7a**): MEH−PPV (37:63 by mole) blend/Ca/Al at various applied voltages.

side contributed from POPD−PPV increases. This is due to the phase separation of the two polymers (Figure 8b). Each phase in the film has a domain size of about 0.2 to 1 μm, which is larger than the thickness of the emitting layer. Thus, each domain becomes an independent pathway for charge transport and the MEH−PPV-rich phase will emit first at the lower voltage since its E_{to} is lower. This lowering in η is due to the nonuniform distribution of OXD groups in the film and to the imbalance of charge injection to different polymer phases.

E. Structure and Performance Relationships. The structures of the copolymers with the OXD moiety on the side chain explored above indicate that: (1) the electron-deficient moieties are well dispersed in the matrix with conjugated main chains to such an extent that the dispersion between them is intrachain in nature; (2) the dispersion of OXD does not lead to an interaction in the ground state and excited state but does allow an energy transfer to occur from the OXD group to the conjugated main chain although not to a great extent. The OXD groups on the interfaces with the electrodes act as hole-blocking and electron-transporting sites, and those in the bulk are able to promote the electron transport as reflected in the increased charge flux as compared to the device with MEHPPV. Such dual roles of OXD groups lead to a presence of optimum content of OXD in the copolymer. Contrary to the increased turn-on voltage by adding an electron-transport layer, the reduced turn-on voltage is due to the incomplete coverage of OXD groups on both electrode surfaces and balanced electron- and hole injections. The optimal OXD content for the device with Ca is lower than that of the device with Al, since the former allows a larger flux of electrons from the cathode than the latter. Its role is quite different from that when used as an electron-transport layer (such as the OXD-containing material, PBD, is introduced), which actually acts as a hole-blocking layer. In addition, this route of design is better than blending the emissive material of PPVs with PBD or OXD-containing PPVs, which could result in no improvement in the efficiency of the devices.

Conclusions and Significance of the Present Route of Molecular Design

It is conclusive that the present route is significantly better than introducing an electron-transport layer (ETL), incorporation of ETL materials by physical blending, and other molecular design routes. It permits a fabrication of single-layer PLED with high brightness, high efficiency, and low turn-on voltage. Its significances are depicted as follows. (1) The electron-transport moiety together with a flexible spacer is incorporated as a side chain of the p-type conjugated main chain; both roles of the side chain and main chain for light emission are retained. (2) The use of phenylene vinylene derivatives with asymmetric and branched substituents and a long spacer provides a solubility for ease of device fabrication as well as amorphous structure to allow efficient mixing of side chains with main chains, such that good dispersion of OXD groups in the copolymers occurs. (3) The copolymerization route permits the adjustment of OXD content in the entire composition range so that a balance of electron- and hole injections can be tuned for various metal cathodes. Compared to the other methods for improving the efficiency of the devices reported in the literature,[9−12] the use of the present copolymers permits an elimination of an electron-transport layer which leads to an increase in turn-on voltage[6b−d] and prevents phase separation between the electron-transporting moiety and the copolymer main chain which is likely to occur in the physical blends.[8b,d] The use of the present design route allows a free adjusting of the OXD content so that an improvement in the efficiency for the device with Ca as cathode for which the required OXD content is lower than that with Al as cathode. This is probably the reason the reported device performance with Ca as cathode does not show significant improvement as OXD is introduced into the side chain.[16a,b]

Acknowledgment. We thank the National Science Council of the Republic of China for financial aid through Project NSC 87-2216-E-007-029.

Supporting Information Available: Instrumentation details, detailed experimental procedures and characterizations for all of the monomers and polymers, and calculation method of external quantum efficiency (PDF). This material is available free of charge via the Internet at http://pubs.acs.org.

JA003135D